Soil Dynamics and Earthquake Engineering 89 (2016) 28–37

Contents lists available at ScienceDirect

Soil Dynamics and Earthquake Engineering

journal homepage: www.elsevier.com/locate/soildyn

Experimental evaluation of vulnerability for urban segmental tunnels subjected to normal surface faulting

Majid Kiani [a,*], Abbas Ghalandarzadeh [b], Tohid Akhlaghi [a], Mohammad Ahmadi [c]

[a] Department of Civil Engineering, University of Tabriz, 29 Bahman Sq., Azadi Ave., Tabriz, Iran
[b] School of Civil Engineering, University College of Engineering, University of Tehran, Engelab Ave, Tehran, Iran
[c] International Institute of Earthquake Engineering and Seismology (IIEES), No. 21, Arghavan St., North Dibaji St., Farmanyeh, Tehran, Iran

ARTICLE INFO

Article history:
Received 31 August 2015
Received in revised form
14 July 2016
Accepted 18 July 2016

Keywords:
Shallow segmental tunnel
Experimental fragility curves
Normal surface faulting
Centrifuge
Physical modeling

ABSTRACT

Faulting is one type of permanent ground displacement (PGD); tunnels are at the risk of damage when they are susceptible to faulting. The present study proposes an experimental approach to create the fragility curves for shallow segmental tunnels in alluvial deposits subjected to normal surface faulting. Centrifuge testing was carried out in order to achieve this purpose. The proposed approach allows evaluation of new fragility curves considering the distinctive features of tunnel geometry and fault specifications. The comparison between the new fragility curves and the existing empirical curves was discussed as well. Compared to tunnels in rock, tunnels in alluvial deposits are more susceptible to failure because of different mechanisms of collapse into tunnel at large exerted PGD.

1. Introduction

The consequences of earthquake may be classified in terms of their direct and indirect effects. The indirect ones are sometimes referred to by economists as more significant. The direct impacts of an earthquake are to be appeared immediately because of its social and physical outcomes.

Indirect effects take into account the system-wide consequences of flow loss from inter-industry relationships and economic sectors [1]. For example, when a metro underground line, classified as a lifeline, suffers damage because of an earthquake, it may impose important indirect effects to human lives and to the operation of a comprehensive transportation system as well. The failure of the Kobe metropolitan line is a typical example of this event [2].

Risk managers, city planners and authorities should be aware of the expected degree of damage for each transportation component exposed to different earthquake scenarios [2]. The reliability of a structural system or lifeline can be considered as the ability of the whole system or its components to perform their required functions under stated conditions for a specified period of time. Because of uncertainties in loading and capacity, this usually includes probabilistic methods and is often done by using indices such as safety index or the probability of failure of a structure [1]. Seismic risk assessment has witnessed remarkable developments in recent decades. A detailed review of this subject has been presented by [3,4].

It is possible to describe the vulnerable components of a structure by using vulnerability and/or fragility functions. One possible convention describes vulnerability functions as the probability of loss (such as social or economic loss) given the level of ground shaking. Fragility curves detect the probability of a structure reaching a certain damage state for a given seismic parameter such as PGA, PGV and PGD (peak ground displacement). Parameters such as PGD (permanent ground displacement) can also be used for fragility curves [2,4,5] the same as for current study.

Previous studies (classified into four following categories by researchers [1,5–7]) have developed several methods that can be applied to create fragility curves,

- empirical method based on the effects of past earthquake damage;
- expert judgment based on direct assessment given by experts;
- numerical method based on the results gained by numerical modeling;
- Experimental method based on the results gained by physical modeling.

Fragility curves can also be derived as a combination of two or more of these methods.

Fragility curves for tunnels are primarily based on expert judgment and empirical or numerical approaches [2,8]. The

* Corresponding author.
E-mail addresses: kiani@tabrizu.ac.ir (M. Kiani), aghaland@ut.ac.ir (A. Ghalandarzadeh), takhlaghi@tabrizu.ac.ir (T. Akhlaghi), mo.ahmadi@iiees.ac.ir (M. Ahmadi).

http://dx.doi.org/10.1016/j.soildyn.2016.07.012
0267-7261/

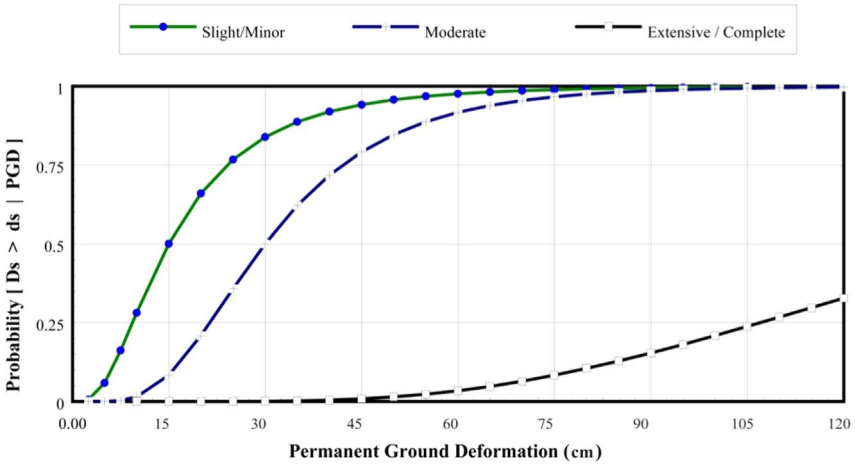

Fig. 1. Tunnel fragility curves for damage states subjected to PGD. Reproduced from [9].

majority of the available fragility curves are given as a function of ground shaking parameters instead of permanent ground displacement. The fragility curves for tunnels suggested by HAZUS use PGD as the seismic parameter [9]. The HAZUS approach [9] is based on judgment and limited empirical data set by [10,11], providing fragility curves both for ground shaking (PGA) and ground failure (PGD). HAZUS fragility curves for permanent ground displacement (PGD) are presented in Fig. 1.

The present study developed a comprehensive experimental approach (centrifuge modeling) to establish fragility curves for shallow light railway tunnels in alluvial deposits. A comparison between proposed fragility curves and existing empirical curves of HAZUS highlights the role of segmental lining and soil conditions effects.

The behavior of segmental tunnels subjected to normal fault displacement was studied by applying PGD under quasi-static conditions. By applying PGD for segmental tunnel, the surrounding soil was physically modeled (using different Input PGDs, fault angles and thickness of soil overburden) in a geotechnical centrifuge. Tunnel damage states for each PGD were determined by using video records from inside of the tunnel. The fragility curves were created as a function of PGD for each tunnel damage state.

2. Deriving fragility curves

2.1. Damage states

The damage states for derivation of fragility curves are defined differently by up-mentioned methods. Damage states for empirical methods are usually based on observation and engineering judgment; however, in numerical methods quantitative criteria are used to define damage states for fragility curves. For existing empirical fragility curves of the tunnels, qualitative damage descriptions were used based on evidence from past earthquakes [2].

Five damage states have been defined qualitatively in HAZUS to derive fragility curves for shallow urban metro tunnels. The main criterion for HAZUS is the fraction through the lining of the tunnel. Previous studies proposed various seismic fragility functions [2,12,13]. Table 1 summarizes existing fragility functions for tunnels related to permanent ground deformation (PGD). HAZUS suggesting a level of damage to tunnels, applied engineering judgment to define the five different damage states caused by PGD as fallow:

- DS1 (none): no damage;
- DS2 (slight/minor): minor cracking of the tunnel liner (damage requires only cosmetic repair) and some falling rock, or slight settlement of the ground at the tunnel portal;
- DS3 (moderate): moderate cracking of the tunnel liner and falling rock;
- DS4 (extensive): major ground settlement at a tunnel portal and extensive cracking of the tunnel liner;
- DS5 (complete): major cracking of the tunnel liner that may include collapse [9].

Table 1
Summary of existing tunnels fragility functions for PGD.

Reference	Methodology	Classification	Intensity Measure Type	Damage States
[9]	HAZUS-engineering judgment and empirical Fragility curves. Log-normal cumulative distribution	Bored/drilled cut and cover	Peak ground acceleration (ground shaking), Permanent ground deformation (ground failure)	None (DS1), Slight/minor (DS2), moderate (DS3), extensive (DS4), complete (DS5) Description: extent of cracking of the liner and settlement of the ground/ rock fall at the portal
[14]	Analytical fragilities for tunnels of the BART project (site specific). Log-normal cumulative distribution	Bored/cut and cover (site specific)	Peak ground acceleration (ground shaking), Permanent ground deformation (fault offset)	Slight/minor (DS1), moderate (DS2), extensive/complete (DS3)
[15]	Preliminary analytical fragility curves	Circular (Bored) (EC8)	Permanent Ground Deformation	Slight/minor (DS1), moderate (DS2), Exceedance of lining capacity Damage Index: Exceedance of lining capacity

Note: DS=damage state.

2.2. Estimation of fragility curve parameters

A fragility curve represents damage likely to happen at a specific damage state with an increase in PGD. The probability of exceeding a damage state at a given level of PGD was estimated for the five limit states. The fragility curves are primarily described by the lognormal probability distribution function. Ground failure is quantified in terms of PGD as:

$$P_f(DS \geq DSi \mid F) = \Phi\left[\frac{1}{\beta}\ln\left(\frac{F}{F_{mi}}\right)\right]$$

Where P_f is the probability of being at or exceeding damage state (DSi), which should be defined in each study for a given PGD. F is the affecting ground motion parameter that is PGD in this study. Φ is the standard cumulative probability function. F_{mi} is the median value of the fault rupture parameter required to cause the i^{th} damage state, and β is the logarithmic standard deviation. The median of F_{mi} is the value of the F at which there is a 50% chance that a component will enter DS.

The results of centrifuge modeling have been used to calculate the fragility curves parameters.

3. Centrifuge tests

3.1. Experimental setup

Fragility curves (indicated in this research) are based on experimental results obtained from centrifuge testing. This section describes the setup used to determine experimental fragility curves and the properties and configurations of the segmental tunnel and fault simulator as well. The tests were carried out by using centrifuge (swinging-basket type beam with 3 m in length) at Tehran University (Iran). The experimental equipment consists of a model box designed to simulate faulting in the centrifuge, segmental tunnels, and recording instrument such as a camera and video system to record the fault propagation through the soil and to catch the occurred phenomenon inside the tunnel.

Fig. 2 shows a typical section with six segments inserted in one ring. The lining of the circular tunnel model was composed of segments with a thickness of 0.9 cm and a width of 2.3 cm. By using scaling law, the dimension of prototype lining has been changed to 35 cm in thick and 115 cm in length. Continuous asbestos cement pipes (with a modulus of elasticity of 20 GPa) were used to model the tunnels. These continuous pipes were precisely sliced to make a segmental lining, then at the location of joints, needed holes were assemble to form the final tunnel lining. Each ring was connected to the other rings by 12 joints in longitudinal directions. Four circumferential joints were also used to connect each segment to be its adjacent one in a ring. It should be noted that the main role of joints in segmental tunnel lining is usually to place segment in its exact location during the installation. Therefore, in tunneling references, the word “pin guide” was used for these joints. The loads and moments in segments are usually transferred through rings contact, not through joints. So, in tests carried out, it was assumed to use hinge joints to simulate a real condition in models. The length and bending stiffness (EI) of joints was modeled based on centrifuge scaling laws in order to make their actions similar to the real ones [16]. It should be noted that, since it is not possible to model the frictional forces between rings, because of some restrictions, some kind of deficiency may occur in modeling process. Since it is not possible to model the force of TBM trust jacks (because of limitation in physical modeling) therefore we encounter constraint in the contact fractional forces.

Since the excavation method was not investigated and modeled

Fig. 2. Typical cross-sections of segmental model tunnel.

In this research, as a result the axial forces cannot be completely developed between each model rings and frictional forces may not exactly scaled as it was in real condition. This deficiency is unavoidable in this kind of physical modeling, but since the main part of this modeling is correctly scaled, it has less effect on tunnel behavior.

Clean sand with D_{50} approximate to 0.3 mm is commonly used in these studies [16–18]. Firoozkuh #161 sand with gradations and other specifications similar to Toyoura sand, was analyzed at Soil Laboratory of Dept. for Civil Engineering of Tehran University. It is commonly used for similar studies in Iran.

Table 2 shows the physical and mechanical specifications of the sand. Soil containing a D_r of 60% was used in all tests. The model construction method was wet tamping of a mixture of 5% water added to dry sand for producing wet homogeneous soil. The soil was poured in 3 cm layers and was tamped to compact it homogeneously throughout the soil box. In order to achieve the desired density, the number of tamps was determined in pilot tests. Finally, taking into account the effect of compaction of above soil layer in density of beneath one, undercompaction method was applied to achieve a fully homogenous specimen [16].

The split box containing the following items was used to model faulting in the centrifuge: soil, a tunnel and a displacement operation system. It was designed for applying both normal and reverse dip-slip faulting for different tests. The soil box was composed of steel and aluminum alloys with 70 cm in length, 50 cm in width and 40 cm in depth. One wall of the box was Plexiglas so that the deformations occurring at different depths could be observed during faulting. A hydraulic jack exerts differential displacement to simulate faulting in specimens. The split box consists of two main parts; first one (the fixed part) called “Foot wall” and the next one called “Hanging wall’ was belong to the movable one. By moving the hanging wall part, faulting can be simulated in each test. Fig. 3 shows a 3D cross-section of the spilt box [16].

Since the tunnel axis is perpendicular to the faulting plane, it inevitably crosses the tunnel. The lining of the model tunnel was segmental and had almost the real conditions. The segments were connected by steel joints that hold segments in order to form a complete or final lining of the tunnel. The failure mechanism subjected to normal faulting was studied. Supports were used in order to minimize the effect of the finite length of the model tunnel to compensate the limited dimensions of the sand box.

Table 2
Physical and mechanical properties of sand.

Name	G_s	e_{max}	e_{min}	D_{50} (mm)	F_C (%)	ϕ	c
Firoozkuh #161 sand	2.658	0.874	0.548	0.27	0	37°	0.0

Note: G_s=specific gravity of solid; e_{max}=maximum void ratio of the soil; e_{min}=minimum void ratio of the soil; D_{50}=median grain size; Fc=content of fines; ϕ=soil frictional angle; c=cohesion of soil.

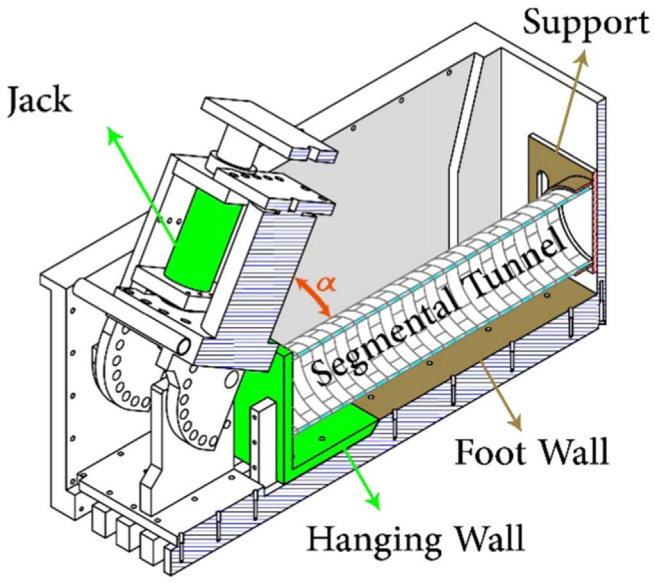

Fig. 3. Split box for modeling fault displacement in a geotechnical centrifuge.

Fig. 4 is a schematic view of the model.

3.2. Scaling law

The proper use of scaling laws is essential for physical modeling [19]. Decreasing the geometric dimensions of the real model does not necessarily create an appropriate model. For modeling, the model materials should meet the proper scaling laws which have been used so far for tunnel modeling in centrifuge by many researchers [20,21]. It must be borne in mind that tunnel lining modeling is the ratio of flexural stiffness per length unit of a model to the prototype based on the coefficient n^4. This indicates the necessity for proper adoption of appropriate materials required for the tunnel lining in the small-scale model. Table 3 shows the scaling factor that was used in this study.

Table 4 shows the model details and their equivalents in real terms by using scaling factors. As it can be concluded, all dimensions (except the thickness) of applied segments were derived by the scaling portion mentioned in scaling law of Table 3 in this modeling, this subject can be interpreted by the importance of flexural stiffness parameter which contains both the modulus of elasticity and tunnel's moment of inertia. So due to the differences between modulus of elasticity for prototype lining (usually made by high strength reinforced concrete) and the asbestos model material, it is possible to achieve the thickness of model segment.

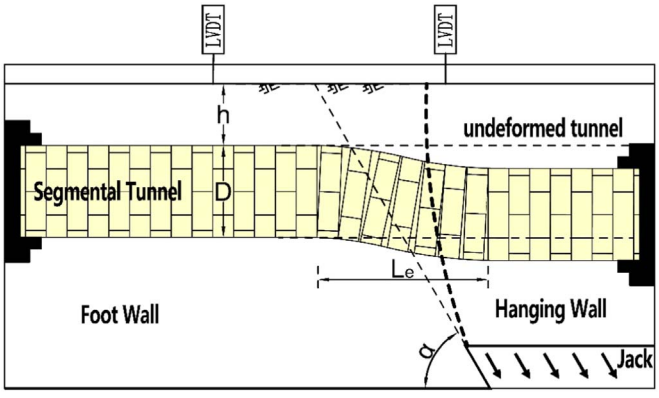

Fig. 4. Schematic view of the model.

Table 3
Scaling factor that was used in this study.

Parameters	Scaling portion	Scaling factor
Length	n	50
Density	1	1
Strain	1	1
Displacement	n	50
Flexural Stiffness	n^4	50^4

Note: n=scaling factor.

Table 4
Scaling dimensions of model (n=50 g).

Parameters	Model	Prototype
Model dimension	70 × 50 × 40 (cm)	35 × 25 × 20 (m)
Length of tunnel	70 (cm)	35 (m)
Tunnel diameter	11.8 (cm)	6.0 (m)
Thickness of segments	0.9 (cm)	0.35 (m)
Width of segments	2.3 (cm)	1.15 (m)
Modulus of elasticity	20 (GPa)	34 (GPa)
Joint's length	8 (mm)	40 (cm)

Note: n=scaling factor.

3.3. Instrumentation

The main purpose of this study was to review the following items: deformation behavior of the tunnel sections, longitudinal tunnel deformation modes, failure mechanisms and surface displacements in response to faulting. LVDT was one of the sensors to measure the vertical displacement of the surface along the tunnel. In order to observe the propagation of faults within the soil and the ground displacement as well, camera was installed in front of the Plexiglas wall. Through this process, the different stages of faulting have also been recorded.

3.4. Test programs

The results of nine centrifuge tests carried out to review the normal surface faulting have been used to make fragility curves. The thickness of overburden soil (h) ratios used (0.75 D, 1.0 D, 1.2 D) was equal to the external diameter of tunnel (D) at faulting angles of 60° and 75°. The variation in parameter gives a better opportunity, in which more applicable fragility curves can be derived. Table 5 gives the details of the tests.

4. Centrifuge tests observations

Relative displacement of faulting causes the tunnel to bend on its longitudinal direction, as a result, can induce damage on tunnel itself and aboveground structures as well. In Section 4.1, Section 4.2 the main damages of the tunnel, but not all of them, in according to their importance and in Section 4.3 creation of sinkholes at ground will be described.

4.1. Failure modes

Understanding the failure modes is one of the most important and applicable results obtained from the faulting tests. It was possible to discern vulnerable areas in the segmental tunnels by determining the failure modes. This may improve the design of new tunnels and the mitigation of existing structures. Failure was not sudden when the tunnel was subjected of normal surface faulting because of the flexible behavior of segmental tunnels. As shown in Fig. 5, when faulting started, a change in tunnel

Table 5
Test programs.

Test	10	32	17	15	14	29	24	23	25
h/D	0.75	1	1.2	0.75	1	1.2	0.75	1	1.2
Angle of fault (degree)	60	60	60	75	75	75	60	60	60
Tunnel diameter (m)	6.0	6.0	6.0	6.0	6.0	6.0	5.0	5.0	5.0

Note: h=height of soil overburden; D=tunnel diameter.

elevation (as a failure) and when faulting continued, the collapse of soil into the tunnel was observed. The collapse of soil into tunnel was due to creation of separation between rings as PGD increased.

Separation is a phenomenon created by tensional component of normal surface faulting. This phenomenon has been occurred in the critical rings located in the faulting zone. Separation at tunnel crown was the result of soil falling through the tunnel. Rings at the section of hanging wall also separated from the tunnel lining; however, the location of these separations was at the bottom of the tunnel, not at the crown. Two or three segmental rings (considered to be critical) at the fault propagation zone were most severely damaged and deformed. The critical rings experienced severe damage, while the damage to the adjacent rings was tolerable. The longitudinal direction of the tunnel bent into an S configuration that schematically shown in Fig. 4.

4.2. Cross sectional deformation

As it is clearly revealed in Fig. 6, during faulting, the critical rings located within the shear zone of fault rupture became ellipsoidal, and while the height of the tunnel cross-section decreased, its width has observed some increase as well. The rings located in the hanging wall were less deformed in comparison to critical rings, while the rings in the footwall were not as deformed as the most severely deformed rings in the hanging wall. As a result, the tunnel in hanging wall would be more vulnerable than in foot wall.

4.3. Sinkholes

As the separation between the critical rings increased, the soil collapsed into the tunnel and finally blocked it. Since the model tunnels were classified as shallow, the opening created at the overburden soil extended to the surface and a large sinkhole appeared on the surface. Since this phenomenon may cause severe damages to above structures adjacent to the tunnel route, it should be put into consideration. Considering the results gained from 6 tests carried out in present study about sinkhole at the ground (Fig. 7) it can be concluded that as the tunnel overburden increased, the sinkhole dimensions decreased. W and L were denoted as the dimensions of sinkhole and were normalized to the tunnel diameter. As indicated in Table 6, it was observed that while the angle of the fault increased, the dimensions of the sinkholes also enhanced.

5. Damage analysis results and evaluation of fragility curves

5.1. Damage states definition

As it mentioned before, three modes of failure can be observed in segmental tunnel linings subjected to normal surface faulting by using geotechnical centrifuge tests. The first mode is longitudinal deformation where changing in slope of the tunnel may disturb its operation. Railway systems are sensitivity to distinct changes in their path; thus, it would be necessary to stop the railway system and repair it. The second mode is cross-sectional deformation perpendicular to the longitudinal axis of the tunnel. This can result from “Ovaling” deformation of a circular tunnel cross-section. The third mode of failure is collapse of soil into the tunnel. In this mode, the separation between rings causes soil to collapse into the tunnel and finally block it. Occurrence of this mode may require comprehensive restoration and rebuilding of the tunnel which is costly and time-consuming. With regard to the above indicated points, five damage states (listed in Table 7) were defined (DS1 to DS5) in present study for segmental tunnel in light railway system subjected to PGD. In DS0, neither damages to tunnel nor changes in its performances were observed in tests.

5.2. Development of damage during faulting

The deformation appeared on the critical section of the tunnel during vertical fault displacement was used to obtain the failure curves. A camera mounted inside the tunnel equipped with a sensor (that recorded fault displacement) was used to provide an image of a vertical fault with a value of 0.1 m inside the tunnel for each step of the imposed faulting. As a sample, Fig. 8 shows the gradual change in the shape of tunnel cross-section for the vertical displacement up to soil collapse for test 14. The PGD denotes the amount of vertical fault displacement and DS indicates the damage state set at that moment, while DS0 shows the absence of displacement in the tunnel lining. As the level of PGD increased, more damage occurred in the tunnel.

The recorded pictures were used as a visual basis for distinguishing of different damages states (DSi). The observed failures were selected to be consistent with the defined damage level. The outcome (presented in Fig. 9) shows the damage curves obtained by analysis of photographs of the inside of the tunnel at PGD step 0.1 m. According to these observations, no damages have occurred when a slight PGD at order of 0.1–0.3 m in different conditions was applied (DS0). This could indicate the tunnel's ability to dissipate the effects of faulting to some extent.

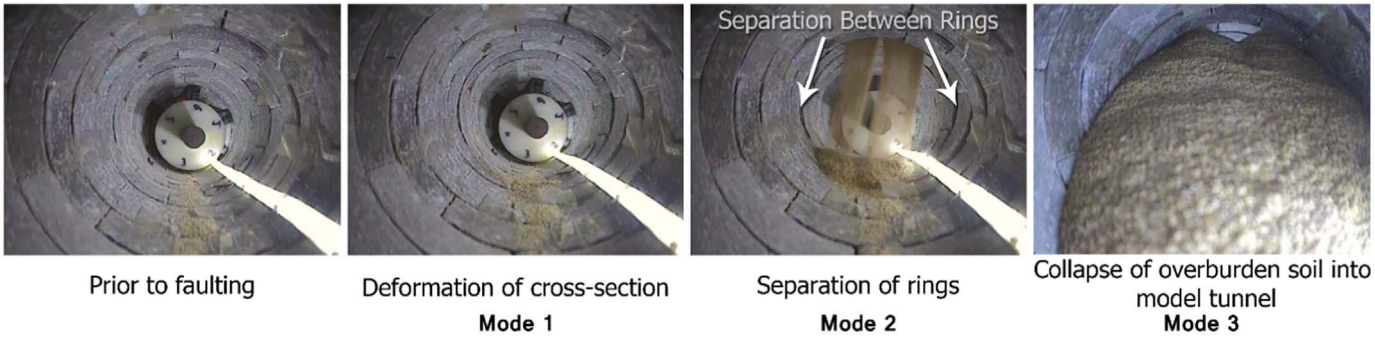

Fig. 5. Cross-sections showing tunnel failure modes.

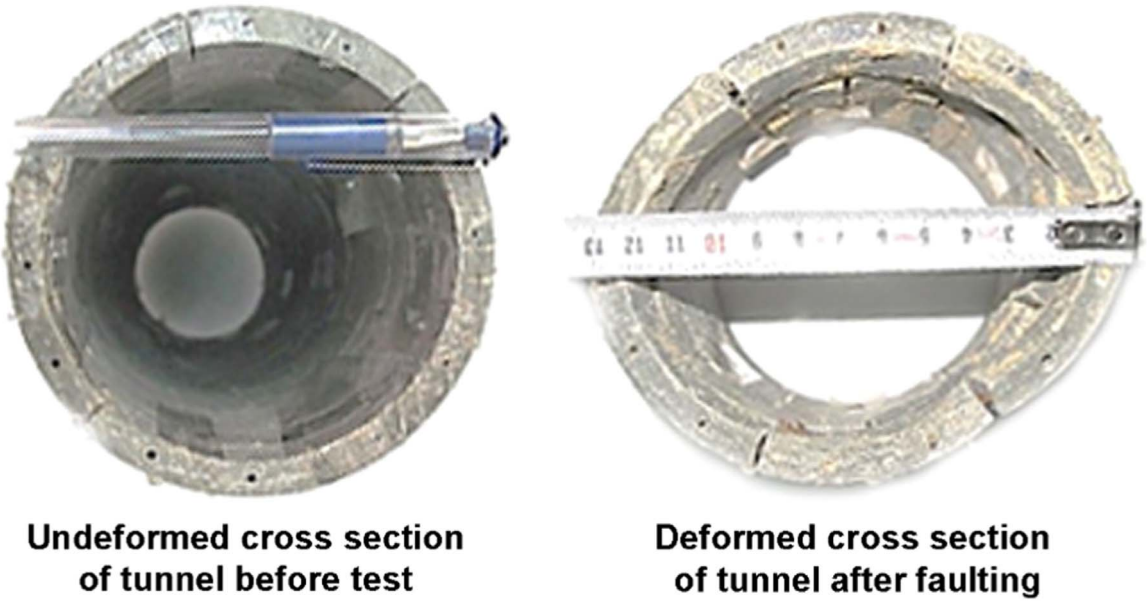

Fig. 6. Cross-sections of tunnel before and after faulting.

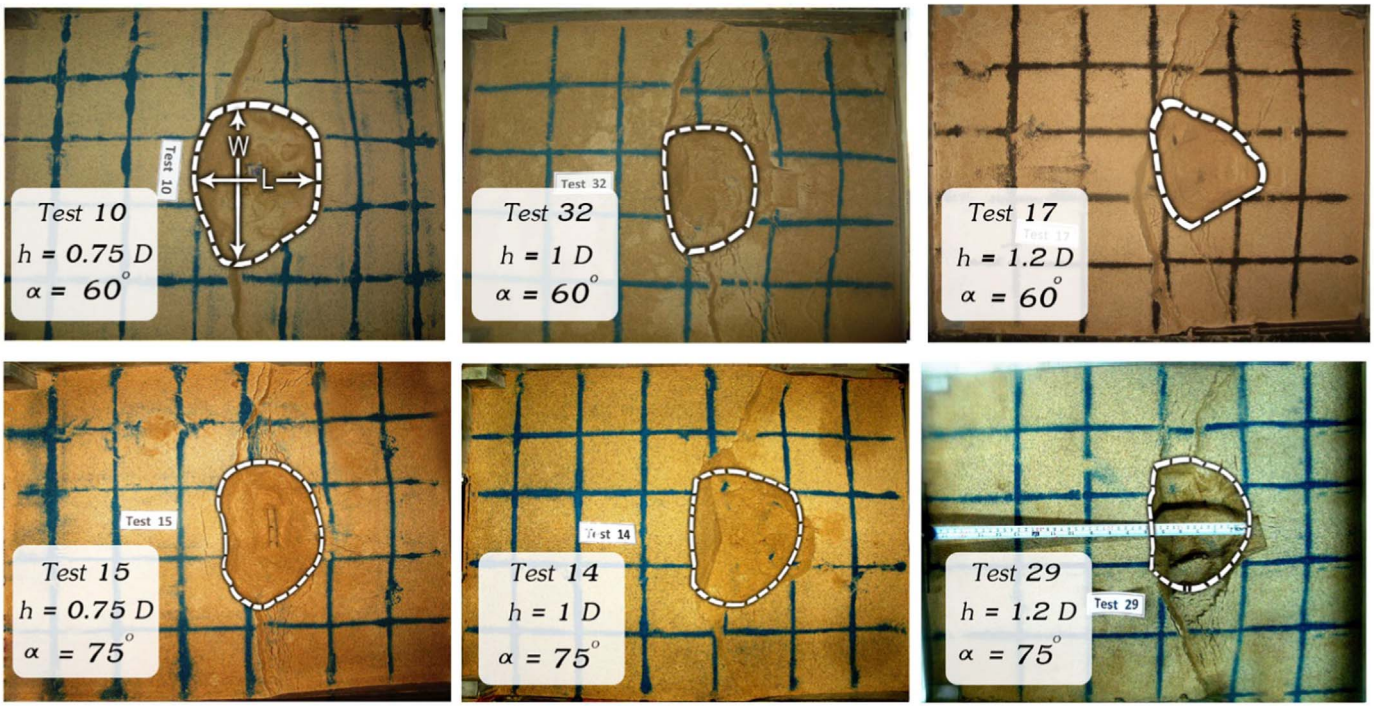

Fig. 7. Sinkholes at ground surface after faulting; W=maximum diameters of sinkhole parallel to the fault plane, L=maximum diameters of sinkhole perpendicular to the fault plane.

Table 6
Dimensions of sinkholes in 6 tests.

Test no.	Fault angle (degrees)	Overburden of soil[a]	Sinkhole dimensions (W × L)[a]
10	60	0.75 D	1.75 D × 1.5 D
32	60	1 D	1.65 D × 1.4 D
17	60	1.2 D	1.5 D × 1.3 D
15	75	0.75 D	1.9 D × 1.3 D
14	75	1 D	1.7 D × 1.2 D
29	75	1.2 D	1.6 D × 1.1 D

Note: D=diameter of tunnel; W=width of sinkhole; L=length of sinkhole.

[a] Normalized to tunnel diameter.

5.3. Fragility curves

As it mentioned in Section 2.2, a fragility curve represents the probability of damage occurring at a specific damage state with an increase in PGD. A log-normal distribution function is usually used to plot the fragility curves. Comparing the results obtained by log-normal and normal distribution function shows there were no significant differences between them. As a common practice, fragility curves are also fitted to the log–normal cumulative distribution functions [22]. The horizontal axis of the fragility curve represents PGD of up to 250 cm applied on the models during experimental testing and the vertical axis represents the probability of damage exceeding at a specific damage state. The study

Table 7
Damage states for segmental tunnels in light railway system subjected to PGD.

Damage state	Description	Performance state
DS0	No damage	Normal operation
DS1	Slight change in tunnel slope in longitudinal direction	Normal operation or a negligible stop in operation with no/negligible repair
DS2	Significant change in tunnel elevation in longitudinal direction	Small pause in operation for repair (low cost)
DS3	Cross-sectional deformation of tunnel (ovaling)	Pause in operation for repair (costly to repair)
DS4	Separation between segmental rings and damage to segmental joints	Pause in operation for restoration
DS5	Failure of segments, tunnel collapse/probable sinkhole at ground	Full tunnel blockage requiring total restoration (very costly to rebuild)

Note: PGD=permanent ground displacement; DS=damage state.

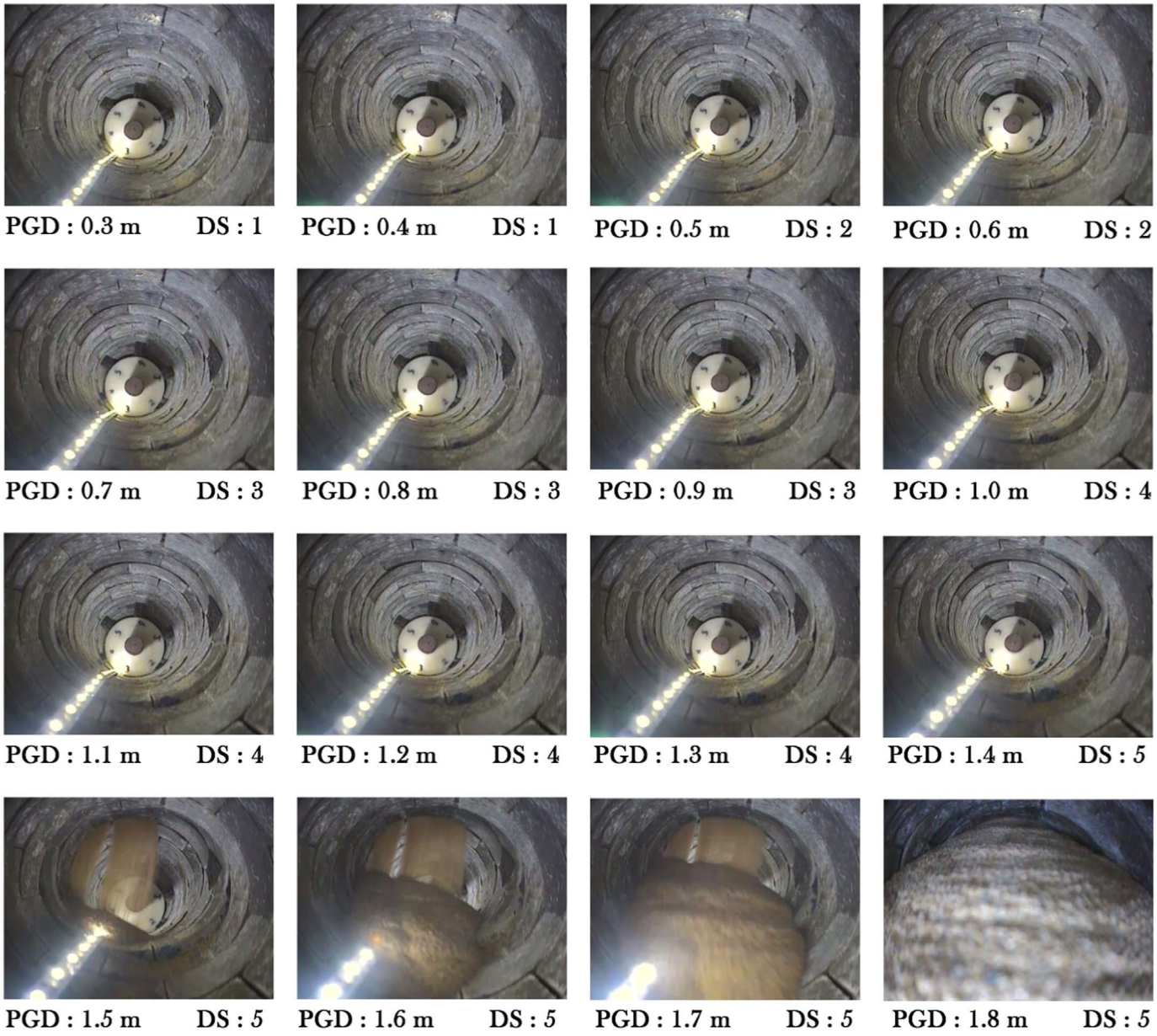

Fig. 8. Progress of tunnel lining deformation and damage state with increase in vertical fault displacement in test 14 (PGD increment: 0.1 m in prototype).

of these curves can lead to better designs of tunnels to withstand faulting. Table 8 shows the PGD values for vertical fault movement in which the soil enters to DS_i. These values were used to derive the fragility curves for DS1 to DS5 as well; the value of DS5 with the most important effect among the other data in which the tunnel was blocked by the collapsing soil and sinkhole was appeared.

Fig. 10 is a basic depiction of derived fragility functions for a segmental tunnel in a light railway system. In addition, Table 9 shows standard deviations (β) and median (F_{mi}) of each damage

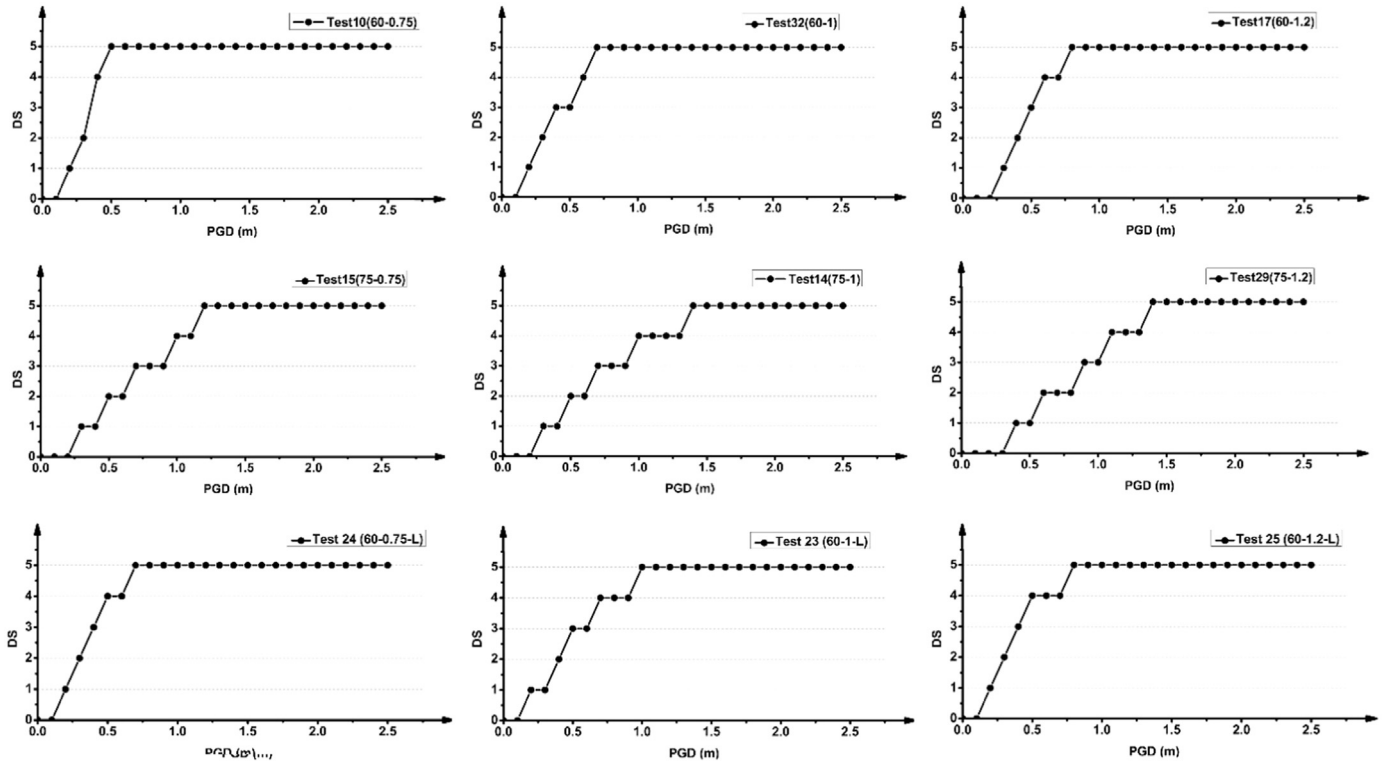

Fig. 9. Damage curve for tests conducted in current study.

Table 8
PGD Values in which tunnel enter DS_i.

Test		10	32	17	15	14	29	24	23	25
PGD (m)	**DS1**	0.2	0.2	0.3	0.3	0.3	0.4	0.2	0.2	0.2
	DS2	0.3	0.3	0.4	0.5	0.5	0.6	0.3	0.4	0.3
	DS3	0.4	0.4	0.5	0.7	0.7	0.9	0.4	0.5	0.4
	DS4	0.4	0.6	0.6	1.0	1.0	1.1	0.5	0.7	0.5
	DS5	0.5	0.7	0.8	1.2	1.4	1.4	0.7	1.0	0.8

Note: PGD=permanent ground displacement; DS=damage state.

Table 9
Standard deviation (β) and median (F_{mi}) of PGD in every DSi.

DS level	1	2	3	4	5
β	0.266	0.270	0.307	0.359	0.350
F_{mi} (m)	0.25	0.40	0.54	0.71	0.94

Note: β=Standard deviation; F_{mi}=median; PGD=permanent ground displacement; DS=damage state.

state curves. F_{mi} is defined as the average value of logarithm of PGDs (in cm) for each DS. For example, F_{mi} of DS5 is calculated equal to 4.49. Also standard deviation (β) of logarithm of PGDs (in cm) for DS5 estimated as 0.35 cm.

5.4. Discussion of derived fragility curves

An important aspect of a fragility curve is to estimate tunnel resistance when it intersects an active fault. Results show that the probability of tunnel performance attaining DS1 is less than 10% for PGD about 15 cm. This represents the ability of a segmental tunnel to deform and dissipate the effect of local displacement at the beginning of faulting. For vertical displacement of 35 cm, the probability of attaining DS1 exceeds 90%.

Reviewing the DS5 fragility curve is also necessary. This curve indicates that relatively large localized fault deformation is required to force total collapse of the lining and collapse of the soil into the tunnel. The probability of total collapse (DS5) is less than 10% for vertical fault displacement of 55 cm and exceeds 90% at

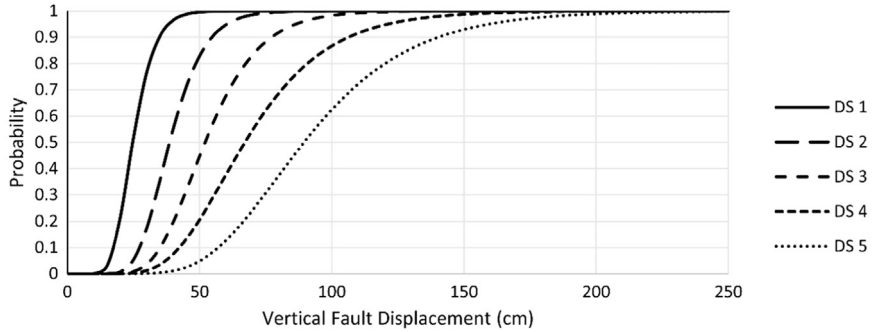

Fig. 10. Fragility curves derived for segmental tunnel lining subjected to PGD.

about 140 cm. Development of an accurate design can be achieved by careful attention to this factor.

5.5. Experimental versus empirical fragility curves

The experimentally-derived fragility curves were compared with the empirical curves proposed by HAZUS [9] based on damage data collected from tunnels that have experienced earthquakes. HAZUS tunnel damage functions were developed using the empirical method [23]. The G&E findings are based partly on earthquake experience data reported by [10,11]. The most significant tunnel damage in the G&E recorded was for tunnels bored in rock [23]. The linings of these tunnels were primarily continuous reinforced concrete (Tanna tunnel in 1930, Izu-Inatori in 1978, Wilson canyon channel in 1971) [11]. It is clear that the behavior of this kind of tunnel may widely different from the tunnels investigated in the present study. Also it should be noted that the number of cases that take into account for deriving fragility curves are few.

Fig. 10 shows the fragility curves derived in this research and Fig. 1 was the fragility functions introduced by HAZUS. Five damage states are introduced by HAZUS. However, the proposed fragility curves by HAZUS indicate three damage states. They combined damage states 1 and 2 and also damage state 4 and 5 to derive three fragility curves. The current study depicts all five damage states as fragility curves in Fig. 10.

The following point can be noticed when the fragility curves of the current study is compared to those of HAZUS:

a) The data of the present research produced by experimental testing in a centrifuge is similar to the empirical fragility curves derived by HAZUS.
b) Most tunnels investigated by HAZUS were bored in rock while in this study the soil tunnel has been used. The behavior of a tunnel in rock is distinct from that of tunnels constructed in soil.
c) In HAZUS report, the available data of segmental tunnel was insufficient. Current modeling shows failure of segmental tunnels caused by normal surface faulting is not sudden and the tunnel lining can tolerate a degree of faulting without any total destruction. A damage level can occur even in a small fault displacement for a continuous lining tunnel. For a certain PGD, the higher probability for DS1–DS3 of HAZUS curves is because the different behaviors of continuous lining and segmental one. Although DS1–DS3 of HAZUS curves are not equal to the same items prepared in current study, but they can be compared with each other; however, DS4–DS5 are widely different. This could be the result of the different mechanisms of collapse in tunnels constructed in soil and in rock and also the effect of segmental lining. For normal surface faulting, major failure and soil collapse inside the segmental tunnel resulted from the opening of spaces between the segmental rings. A continuous lining shows a different pattern of crack enlargement. For rock tunnels because of its tensile strength, a large separation in the lining (after cracking) is required to collapse and block it. However for soil tunnels, it is different. Therefore, it is reasonable to observe a lower probability for DS4–DS5 in HAZUS comparing the current study.

6. Design recommendations

Design standards and guidelines generally recommend avoidance of tunnel construction in fault zones. The Japanese Standard Specifications for Shield Tunneling [24] suggests consideration of the effect of faulting on tunnel lining, particularly in the longitudinal direction, in addition to the effects of earthquake vibration. It does not contain any design recommendations about the effects of fault rupture. For a structure crossing an active fault [25], recommends a “general design philosophy that is accommodating expected fault displacements, and allow repair of damaged lining afterwards. Design strategies for tunnels crossing active faults depend on the magnitude of displacement and the width of the zone over which that displacement is distributed”.

The results of the current study suggest that the magnitude of faulting can significantly affect the damage level to the tunnel and also above-ground structures. The fragility curves show that different damage scenarios should be taken into account during the design of tunnel lining. With the occurrence potential of different amount of fault displacement in a real case, designers should choose the best damage scenario to design. For instance, if the probability of large displacement is low, designing tunnel to the level of DS5 (total collapse of tunnel) may not economical.

The current study also recorded formation of a sinkhole in a tunnel subjected to large displacement caused by normal faulting. The possible of a large fault displacement should be also considered through lining design. Also all practicable actions to prevent the soil collapsed to the tunnel are strongly recommended. As an initial recommend, for instance, grouting the soil above the tunnel in case of shallow tunnels can decrease the probability of total collapse of tunnel and sinkhole creature.

“If fault movements are small i.e. less than a few inches and or distributed over a relatively wide zone, it is possible that the tunnel may be designed to accommodate the fault displacement by providing articulation of the tunnel liner with ductile joints. This allows the tunnel to distort into an S-shape through the fault zone without rupture” [25]. Although this recommendation can be interpreted by derived fragility curves of DS1 to DS4 that is before total collapse.

It should be noted that these derived fragility curve are based on some physical modeling tests in centrifuge with some restrictions indicated before in Section 3, so by using more other tests in different situations and also by using numerical analysis [26–28] the fragility curves can be derived more accurate.

7. Conclusions

- Experimental fragility curves were derived for segmental tunnels subjected to PGD caused by surface faulting.
- Based on defined five damage states (DS1–DS5) in present study, five fragility curves were derived.
- These fragility curves were compared and discussed with the HAZUS fragility curves.
- Fragility curves DS1-2 and DS3 are almost similar to the curves of the current study and can be compared; however, DS4-5 of HAZUS is widely different from the corresponding curve of the current study due to the distinct differences in the behaviors of the continuous lining and segmental one.
- The differences between the fragility curves of segmental tunnels derived by this study and HAZUS methodology resulted from the distinct behaviors of the linings and of the surrounded formations. Tunnels in alluvial deposits are more susceptible to damage than rock due to the different mechanisms of collapse into it at large PGD.
- Segmental tunnel lining has the ability of more deformation to dissipate the effects of faulting than continuous one.
- Fragility curves can help in the design of segmental tunnels that intersect faults. These fragility curves can be useful in risk assessment studies for urban tunnels management.

Acknowledgments

The authors would like to thank Ghaem Engineering Institute and also Dr. Rohollah Amirabadi, Mr. MohammadAli Salimi, Mr. Majid Hedayati and Mr. Mahdi Mahdavi for their valuable supports and corporations.

References

[1] Kalantari A. Seismic Risk of Structures and the Economic Issues of Earthquakes. InTech 2012. http://dx.doi.org/10.5772/50789 ⟨http://www.intechopen.com/books/earthquake-engineering/seismic-risk-of-structures-and-the-economic-issues-of-earthquakes⟩ [30.08.15].
[2] Argyroudis S, Pitilakis KD. Seismic fragility curves of shallow tunnels in alluvial deposits. Soil Dyn Earthq Eng 2012;35:1–12.
[3] Calvi GM, Pinho R, Magenes G, Bomme JJ, Restrepo-Vélez L, Crowley H. Development of seismic vulnerability assessment methodologies over the past 30 years. J Earthq Technol 2006;43:75–104.
[4] Pitilakis K, Crowley H, Kaynia A, editors. SYNER-G: typology definition and fragility functions for physical elements at seismic risk, buildings, lifelines, transportation networks and critical facilities, series: geotechnical, geological and earthquake engineering, vol. 27. The Netherlands: Springer; 2014 ISBN: 978-94-007-7871-9.
[5] Kaynia AM, editor. Guidelines for deriving seismic fragility functions of elements at risk: buildings, lifelines, transportation. Ispra(Va) Italy: Eurpoean Commission Joint Research Centre; 2013. http://dx.doi.org/10.2788/19605 Syner-G reference report 4.
[6] Choi E, DesRoches R, Nielson B. Seismic fragility of typical bridges in moderate seismic zones. Eng Struct 2004;26:187–99.
[7] Mackie K, Stojadinovic B. Fragility curves for reinforced concrete highway overpass bridges. In: 13th world conference on earthquake engineering, paper no. 1553. ⟨http://www.iitk.ac.in/nicee/wcee/article/13_1553.pdf⟩; 2004 [30.08.15].
[8] Wang ZZ, Zhang Z, Gao B. The seismic behavior of the tunnel across active fault. In: Proceedings of the 15th world conference on earthquake engineering. Lisbon, Portugal. ⟨http://www.iitk.ac.in/nicee/wcee/article/WCEE2012_0779.pdf⟩; 2012 [30.08.15].
[9] FEMA (Federal Emergency Management Agency) Multi-hazard Loss Estimation Methodology: Earthquake Model. HAZUS MH-MR5, FEMA Mitigation Division, Washington D.C. ⟨http://www.fema.gov/media-library-data/20130726-1715-25045-2065/hazus_mr4_earthquake_tech_manual.txt⟩; 2010 [30.08.15].
[10] Dowding CH, Rozen A. Damage to rock tunnels from earthquake shaking. J Geotech Eng Div 1978;104:175–91.
[11] Owen GN, Scholl RE. Earthquake engineering analysis of a large underground structures. Washington D.C: Federal Highway Administration and National Science Foundation; 1981.
[12] J. Eidinger. Seismic fragility formulations for water systems, sponsored by the American Lifelines Alliance, G&E Engineering Systems Inc., web site, 2001.
[13] Corigliano M. Seismic response of deep tunnels in near-fault conditions. pH.D. dissertation, Politecnico di Torino, Italy; 2007.
[14] Salmon M, Wang J, Jones D, Wu C. Fragility formulations for the BART system. Advancing Mitigation Technologies and Disaster Response for Lifeline Systems; 2003. p. 183–92. ⟨http://dx.doi.org/10.1061/40687(2003)19⟩ [30.08.15].
[15] Argyroudis S, Pitilakis KD. Development of vulnerability curves for circular shallow tunnels due to ground shaking and ground failure. In: Landslides: from mapping to loss and risk estimation; 2007. p. 175–84. LESSLOSS report no. 2007/01, IUSS Press, ISBN: 978-88-6198-005-1.
[16] Kiani M, Akhlaghi T, Ghalandarzadeh A. Experimental modeling of segmental shallow tunnels in alluvial affected by normal faults. Tunn Undergr Space Technol 2016;51:108–19. http://dx.doi.org/10.1016/j.tust.2015.10.005.
[17] Tsinidis G, Pitilakis K, Madabhushi G, Heron C. Dynamic response of flexible square tunnels: centrifuge testing and validation of existing design methodologies. Geotechnique 2015. http://dx.doi.org/10.1680/geot.SIP.15.P.004.
[18] Sabermahani M, Ghalandarzadeh A, Fakher A. Experimental study on seismic deformation modes of reinforced-soil walls. Geotext Geomembr 2009;27:121–36. http://dx.doi.org/10.1016/j.geotexmem.2008.09.009.
[19] Muir-Wood D. Geotechnical Modelling. New York; Spon Press; 2004, ISBN-13: 978–0419237303, Isbn-10: 0419237305.
[20] Lanzano G, Bilotta E, Russo G, Silvestri F, Madabhushi SPG. Centrifuge modelling of seismic loading on tunnels in sand. Geotech Test J 2012;35(6):854–69.
[21] Cilingir U, Madabhushi SPG. A model study on the effects of input motion on the seismic behaviour of tunnels. Soil Dyn Earthq Eng 2011;31:452–62.
[22] Heidary-Torkamani H, Bargi K, Amirabadi R. Seismic vulnerability assessment of pile-supported wharves using fragility curves. Struct Infrastruct Eng: Maint Manag Life-Cycle Des Perform 2013. http://dx.doi.org/10.1080/15732479.2013.823453.
[23] G&E. NIBS earthquake loss estimation methods. G&E Engineering Systems; 1994.
[24] Japan Society of Civil Engineering (JSCE). Standard specifications for tunneling – 2006: shield tunnels; 2006.
[25] Hashash YMA, Hook JJ, Schmidt B, Yao JIC. Seismic design and analysis of underground structures. Tunn Undergr Space Technol 2001;16:247–93.
[26] ASCE. Committee in gas and liquid fuel lifelines guidelines for the seismic design of oil and gas pipeline systems. New York: Technical Council on Lifeline Earthquake Engineering, ASCE; 1984.
[27] Anastasopoulos I, Gerolymos N, Drosos V, Georgarakos T, Kourkoulis R, Gazetas G. Behaviour of deep immersed tunnel under combined normal fault rupture deformation and subsequent seismic shaking. Bull Earthq Eng 2008;6(2):213–39.
[28] Anastasopoulos I, Gazetas G. Analysis of cut-and-cover tunnels against large tectonic deformation. Bull Earthq Eng 2010;8(2):283–307.